Original Research

Improved osteogenesis in rat femur segmental defects treated with human allograft and zinc adjuvants

Deboleena Kanjilal[1,2], Christopher Grieg[1,2], Maya Deza Culbertson[1], Sheldon S Lin[1], Michael Vives[1], Joseph Benevenia[1] and J Patrick O'Connor[1]

[1]Department of Orthopaedics, Rutgers-New Jersey Medical School, Newark, NJ 07103, USA; [2]School of Graduate Studies, Rutgers-Newark Health Science Campus, Newark, NJ 07103, USA

Corresponding author: J Patrick O'Connor. Email: oconnojp@njms.rutgers.edu

Impact statement

Orthopedic surgeries requiring large amounts of bone graft often use allograft from cadaver bone. Allograft is processed after collection to reduce immunogenicity and infectious agents. However, allograft processing significantly reduces allograft osteogenic capacity. Adjuvants that can improve the osteogenic properties of processed allograft would be expected to improve the clinical efficacy of the modified allograft. We investigated zinc as an adjuvant to increase the osteogenic capacity of human allograft. Zinc is a trace metal normally found in bone, and exogenous zinc can promote bone fracture healing. Here, we show that the use of zinc as an allograft adjuvant improves allograft osteogenic capacity. Zinc dose and solubility were evaluated using different forms of allograft in a well-established rat femur segmental defect model. Restoring the osteogenic capacity of processed allograft with addition of zinc is expected to improve the clinical performance of allograft and improve patient care.

Abstract

Bone allograft is widely used to treat large bone defects or complex fractures. However, processing methods can significantly compromise allograft osteogenic activity. Adjuvants that can restore the osteogenic activity of processed allograft should improve clinical outcomes. In this study, zinc was tested as an adjuvant to increase the osteogenic activity of human allograft in a *Rag2* null rat femoral defect model. Femoral defects were treated with human demineralized bone matrix (DBM) mixed with carboxy methyl cellulose containing $ZnCl_2$ (0, 75, 150, 300 μg) or Zn stearate (347 μg). Rat femur defects treated with DBM-$ZnCl_2$ (75 μg) and DBM-Zn stearate (347 μg) showed increased calcified tissue in the defect site compared to DBM alone. Radiograph scoring and μCT (microcomputed tomography) analysis showed an increased amount of bone formation at the defects treated with DBM-Zn stearate. Use of zinc as an adjuvant was also tested using human cancellous bone chips. The bone chips were soaked in $ZnCl_2$ solutions before being added to defect sites. Zn adsorbed onto the chips in a time- and concentration-dependent manner. Rat femur defects treated with Zn-bound bone chips had more new bone in the defects based on μCT and histomorphometric analyses. The results indicate that zinc supplementation of human bone allograft improves allograft osteogenic activity in the rat femur defect model.

Keywords: Zinc, bone regeneration, allograft, *Rag2*, rat

***Experimental Biology and Medicine* 2021; 246: 1857–1868. DOI: 10.1177/15353702211019008**

Introduction

Treating large bone defects remains a challenging problem for surgeons.[1,2] Healing of large bone defects is associated with delayed healing and often requires multiple surgeries.[3] Large bone defects are commonly treated by filling the defect void with bone graft. Bone autograft is superior to other graft materials as autograft is living, recipient-sourced material that does not cause an immunogenic response and has osteo-inductive and osteo-conductive properties.[4] If autograft cannot be used or only a limited amount is available, cadaveric bone allograft such as bulk bone, morselized bone chips, or demineralized bone matrix (DBM) can be used as substitutes.[5] Allograft is processed to eliminate potential infectious agents, reduce immunogenicity, and provide specific handling characteristics. Allograft bone chips promote bone formation at the defect site, by providing an osteoconductive surface for bone formation. In contrast, DBM can provide growth factors to promote an osteo-inductive response.[6]

Allograft has a substantial safety record and is often superior to xenograft and synthetic graft materials when promoting healing.[7] However, a significant proportion of bone defects treated with allograft do not heal properly.[8–14] Thus, methods that can improve the efficacy of allograft are desirable.

In prior work, we demonstrated that zinc salts and other insulin-mimetic metal salts can promote bone regeneration in rats.[15,16] Therefore, we hypothesized that zinc could be a possible osteogenic adjuvant for bone allograft.[17] We tested this hypothesis by adding different zinc salts to commonly used DBM and cancellous bone chip allograft and evaluated the zinc-allograft for osteogenic activity in a rat femoral defect model. To begin understanding how zinc may affect the bone healing environment, the effects of different zinc concentrations and zinc salts on the proliferation and viability of murine preosteoclast RAW264.7, osteoblast MC3T3-E1, and chondrocyte ATDC5 cell lines were measured. The experimental results indicate that adding zinc increased the osteogenic activity of human allograft.

Materials and methods

Animal surgeries

Femoral defects were made in the right femur of male 12-week-old *Rag2* null rats (485 ± 68 g, Envigo, USA) as described previously (Figure 1).[18–20] Rats were anesthetized with 3% isoflurane in O_2 (2 L/min) and maintained in 2% isoflurane in O_2 (2 L/min) during surgery. Rats were treated with 22.7 mg/kg of enrofloxacin and 1 mg/kg of slow-release buprenorphine by intramuscular and subcutaneous injection, respectively. Right hind limbs were prepared for surgery and a 2 cm skin incision was made along the anterolateral aspect of the thigh. Soft tissue was bluntly dissected to expose the lateral femur. The fixator was placed on the right femur and secured in place with two proximal and two distal screws. A 4 mm defect was created at the diaphysis using a dental saw. Debris was removed by saline irrigation. Each defect was then filled with 60 mg of allograft containing DBM only, DBM-$ZnCl_2$, DBM-Zn stearate, bone chips, or Zn-bound bone chips (Supplemental Table 1). Soft tissue and skin were closed in layers with 4–0 resorbable sutures. Rats were treated postoperatively with topical antibiotic ointment and intramuscular injections of 22.7 mg/kg enrofloxacin for two days postsurgery. All operative procedures were approved by the New Jersey Medical School Institutional Animal Care and Use Committee.

Preparing the DBM and bone chips

For each rat, 60 mg DBM was mixed with 0.1 ml of 2% carboxy methyl cellulose dissolved in saline and containing 0, 75, 150, or 300 µg of $ZnCl_2$. The DBM-Zn mixture was then molded in 1 cm^3 tuberculin syringes, irradiated, and frozen prior to surgery. During surgery, 0.1 cm^3 (4.7 mm diameter × 4 mm long) of the molded DBM-Zn was placed in the defect site.

In addition to $ZnCl_2$, water insoluble Zn stearate also was evaluated for osteogenic activity when mixed with DBM. Using the apparent optimal dose of $ZnCl_2$, a molematched amount of Zn stearate (347 µg, 0.55 µmol) was mixed with 60 mg of DBM in 2% carboxy methyl cellulose and processed as described earlier.

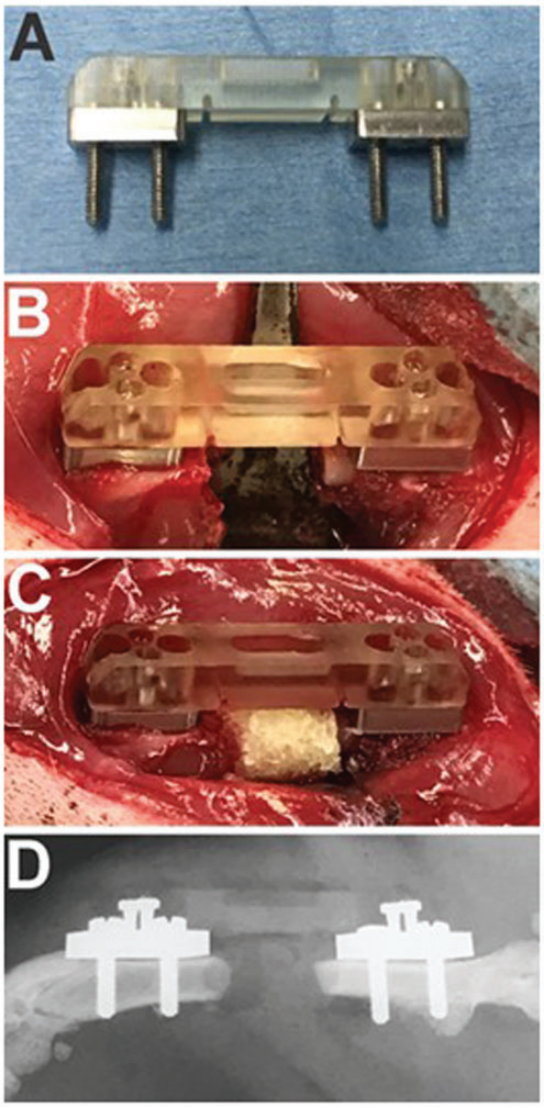

Figure 1. The femoral segmental defect model. A Guldberg fixator (a), a fixator attached to a rat femur with a segmental defect (b), the defect filled with DBM (c), and a postoperative radiograph (d) are shown. (A color version of this figure is available in the online journal.)

Cancellous bone chips (0.2–1.0 mm; Spine Frontier, Miami, FL, USA) were soaked in either Tris-buffered saline (TBS; 0.05 M Tris-Cl, 0.15 M NaCl, pH 7.6) containing 0 or 0.1% $ZnCl_2$ for 30 min at room temperature. Chips were then washed five times with a large excess of TBS. The TBS was carefully aspirated after each wash. Moreover, 60 mg of the Zn-bound bone chips were then mixed with 0.1 ml of 2% CMC, loaded into a 1 cm^3 syringe, irradiated, and frozen prior to surgery.

In vitro Zn binding and retention assays

Allograft bone chips were incubated in TBS containing different concentrations of $ZnCl_2$ (0, 0.01%, 0.1% and 1%) for 24 h to evaluate the effect of different zinc concentrations on zinc adsorption. To measure time-dependent adsorption of

zinc to cancellous bone chips, 0.2 g of bone chips were incubated in 10 ml of 1% $ZnCl_2$ for 0.5, 3, 24, 48, and 96 h. Control bone chips were incubated in TBS for 24 h. To measure zinc retention, bone chips were soaked in 0.1% $ZnCl_2$ for 30 min, washed 5× with TBS and then 0.2 g aliquots of the zinc-bound bone chips were incubated in 10 ml of TBS at room temperature with gentle shaking. Zinc-treated chips were collected at 0, 24, and 48 h and at seven days for analysis.

Bone chips were quickly washed 5× with TBS and assayed for bound Zn by inductively coupled plasma mass spectrometry (ICP-MS). The bone chips were dissolved in 3 ml of concentrated nitric acid (40°C for 4 h), and 50 µl aliquots of the acid extracts were diluted in 4.95 ml of water for ICP-MS analysis. ICP-MS was conducted using an Agilent ICP-MS 7900 (Agilent Technologies, Santa Clara, CA, USA) by the Environmental Core Facilities at the New Jersey Institute of Technology (Newark, NJ, USA).

Radiograph scoring

Rats were serially radiographed every 2 weeks beginning on the day of surgery and continuing until the experimental endpoint at 12 weeks after surgery. Radiographs were obtained either using a Faxitron MX-20 (Hologic, Tucson, AZ, USA) and MinR-2000 mammography film (Kodak, Rochester, NY) or, later in the study, using a Kubtec XPERT 80 digital radiography cabinet (Kubtec Scientific, Stratford, CT, USA). Rats were anesthetized prior to radiographic examination with ketamine (60 mg/kg, intramuscular injection). A lateral view of each femur was obtained by placing the rat supine on the radiographic plate or detector. Six observers blinded to treatments and time points performed a qualitative assessment of the radiographs using a numerical scoring system ranging from 0 (no new bone formation) to 6 (bridging of the defect site; Supplemental Figure 1). The scoring system was based on prior studies measuring bone formation in critically sized defects.[21,22] Observer scores were compared using nested *t*-tests to account for repeated assessments of each radiograph. Agreement between observers when rating any one radiograph was good based on the intraclass correlation coefficient (0.851).

Microcomputed tomography

Calcified tissue in and around the femur defect of all rats euthanized at 12 weeks after surgery was measured using microcomputed tomography (µCT). Femurs were resected, fixed in 10% neutral buffered formalin for seven days at room temperature, and placed in 70% ethanol before scanning. Prior to scanning, all metal components from each sample were removed to prevent X-ray beam artifacts. Samples were scanned at 70 kV, 142 µA, 12 µm voxel size, frame averaging of 4, and a 0.4 rotation step using a Bruker Skyscan 1275 scanner (Bruker Corp., Billerica, MA, USA) with a 1 mm aluminum filter. Images were reconstructed into a three-dimensional volume using NRecon software (Bruker Corp.). After reconstruction, images were segmented using CTAn software (Bruker Corp.). Grayscale values between 47 and 255 were assigned as bone (calcified tissue) for all specimens. The bone volume of the mid-diaphysis region was measured for each specimen. The mid-diaphysis was defined as the calcified tissue between the proximal and distal screw holes nearest the defect margins.

Histology and histomorphometry

Femurs were embedded in polymethylmethacrylate as described previously.[23,24] Embedded samples were cut into longitudinal sections using a low-speed diamond saw (Isomet 11–1180 Low Speed Saw; Buehler Ltd., Evanston, IL, USA) of approximately 300 µm thickness, ground using a Handimet 2 Roll Grinder (Buehler Ltd.) to approximately 150 µm, and polished on a rotating wheel (Ecomet III polisher/grinder, Buehler Ltd.) with aluminum oxide particles. The sections were glued to a 1″ × 3″ plexiglass slide, ground to a thickness of approximately 50–100 µm and polished to remove any residual surface scratches. The slides were stained with a combination of Stevenel's blue and Van Gieson's picrofuchsin, which stains mineralized tissue orange to red, cartilage and proteoglycan-rich tissues deep blue, and other soft tissues lighter shades of blue.[23]

Histomorphometry analysis was performed using Osteomeasure (OsteoMetrics Inc., Decatur, GA, USA). The quantitative analysis of new bone area was performed using a modified version of techniques described by Harten *et al*.[25] Area of new bone formed in the mid-diaphysis was measured.

In vitro cell proliferation and viability assays

To assess zinc effects on cell proliferation, ATDC5, MC3T3-E1, and RAW264.7 cells were plated in 24-well dishes at 1000 cells per well and cultured overnight in complete media (Dulbecco's Modified Eagle's medium with 10% fetal bovine serum and 1% penicillin/streptomycin) before replacing the media with complete media supplemented with 0, 30, 100, or 300 µM of $ZnCl_2$. Both non-adherent and adherent cells were collected after additional four or seven days in culture. Adherent cells were detached with 0.25% trypsin and combined with the non-adherent fraction (the culture media). Cells were collected by centrifugation, the cell pellet was resuspended with 4% trypan blue, and viable (trypan blue negative) cells were counted using a hemocytometer.

To assess zinc effects on cell viability, ATDC5, RAW264.7, and MC3T3-E1 cells were plated in 24-well dishes at 5000 or 1000 cells per well, for the day 2 and day 7 timepoints, respectively, and cultured overnight in complete media before replacing the media with complete media supplemented with 0, 100, or 300 µM of zinc acetate, zinc chloride, zinc citrate, or zinc sulfate. Cells were collected as described previously after additional two or seven days in culture. The numbers of live and dead cells were counted using a hemocytometer. Percent viability was calculated using the number of viable (trypan blue negative) cells divided by the total number of viable and non-viable (trypan blue positive) cells. Three independent replicates were analyzed for each cell line, time point, and treatment.

Statistical analysis

Most statistical analyses were performed using SigmaPlot (v12.5, Systat, San Jose, CA, USA). An *a priori* estimate for sample size determined that a cohort size of seven rats was necessary to detect a 50% difference in mean values between four cohorts with an expected standard deviation of 25% and at a P value of 0.05 with statistical power of 0.8. Parametric data were tested for significance using one-way analyses of variance (ANOVAs) followed by *post hoc* Holm–Sidak corrected t-tests for multiple groups or t-tests for experiments with only two groups. The intraclass correlation coefficient for radiograph scoring was determined using IBM SPSS (v27.0.1.0, Armonk, NY, USA). Radiograph scores were compared between treatments using a nested t-test (GraphPad Prism v9.1; GraphPad Software, LLC, San Diego, CA, USA).

Results

Effects of $ZnCl_2$ mixed with DBM on bone formation

Rat femur defects treated with DBM-$ZnCl_2$ (75 μg) showed improved osteogenesis within the defect. Radiographs of the healing femurs six weeks after surgery appeared to have more radiographic dense material within the defects treated with DBM-$ZnCl_2$ (75 μg) as compared to defects treated with DBM only (Figure 2(a) to (f)). Radiograph scoring also showed significantly improved osteogenesis in rat femur defects treated with DBM-$ZnCl_2$ (75 μg) as early as six weeks after surgery compared to rat femur defects treated with DBM only (nested t-test, $P = 0.019$; Figure 2 (g)). Consistent with the plain radiographic imaging, new bone was apparent in rat femur defects treated with DBM-$ZnCl_2$ (75 μg) by μCT imaging at six weeks after surgery (Figure 2(j)).

Histological examination of the rat femur defects at 12 weeks after surgery also showed apparently more bone formation in rat femur defects treated with DBM-$ZnCl_2$ (75 μg) as compared to DBM only (Figure 2(h) and (i)). Non-calcified remnants of DBM were evident in the defects treated with DBM-$ZnCl_2$ (75 μg).

Effect of Zn stearate mixed with DBM on bone formation

Femur defects treated with DBM-Zn stearate (347 μg) showed radiographic evidence of new bone formation as early as four weeks postsurgery. As shown in Figure 3(a) to (f), the amount of bone formed in the defect site over 12 weeks appeared greater in the rat treated with DBM-Zn stearate (347 μg) as compared to the rat treated with DBM only. DBM-Zn stearate (347 μg)-treated defects also had significantly higher radiographic scores compared to the rats treated with DBM only at six weeks (nested t-test, $P = 0.028$, not shown) and eight weeks postsurgery (nested t-test, $P = 0.024$, Figure 3(g)).

Femurs collected from rats after 12 weeks of healing were analyzed by μCT followed by histological examination (Figure 4). A reconstructed μCT image of a defect

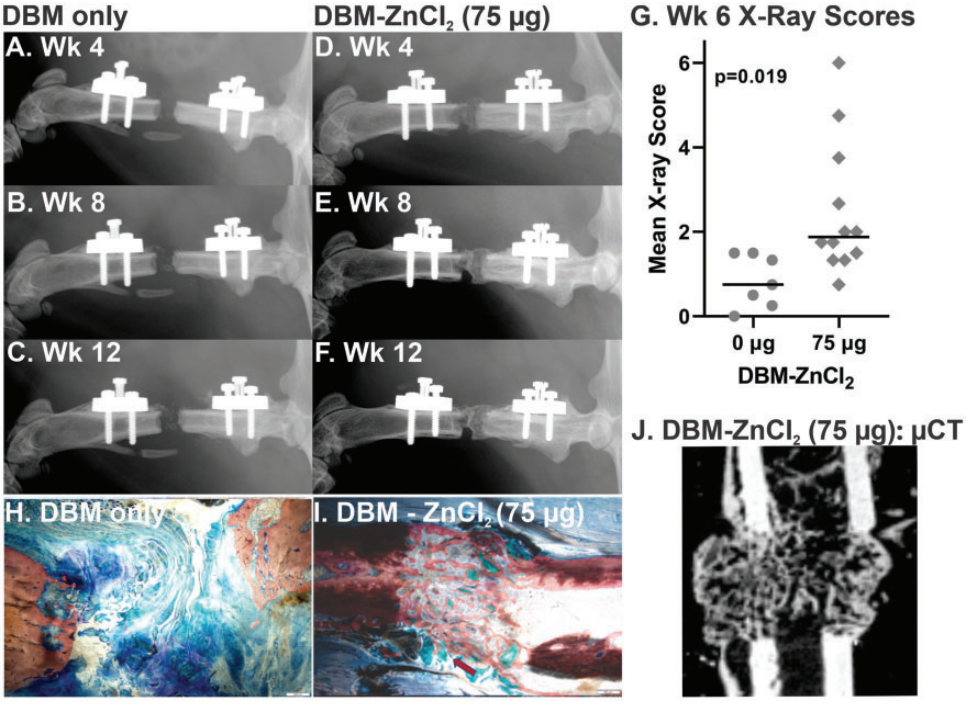

Figure 2. Improved femur defect osteogenesis in rats treated with DBM and $ZnCl_2$. Radiographs at six weeks after surgery from (a to c) a femur defect treated with DBM only (control) and (d to f) a femur defect treated with DBM-$ZnCl_2$ (75 μg) at weeks 4, 8, and 12 postsurgery are shown. (g) Radiograph scores at six weeks after surgery for femur defects treated with DBM-$ZnCl_2$ (75 μg) were significantly higher than femur defects treated with DBM only ($P = 0.019$, nested t-test). Points represent the mean X-ray score for each animal. The horizontal bars show the median for each cohort. Femur histological sections stained with Stevenel's blue and van Gieson's picrofuchsin are shown for defects treated with DBM containing (h) 0 or (i) 75 μg of $ZnCl_2$. The red arrow indicates DBM remnants. Mineralized tissue is stained red. The scale bar in lower right corner is 500 μm. (j) μCt image of rat femur defect treated with DBM- $ZnCl_2$ (75 μg). μCt: microcomputed tomography; DBM: demineralized bone matrix. (A color version of this figure is available in the online journal.)

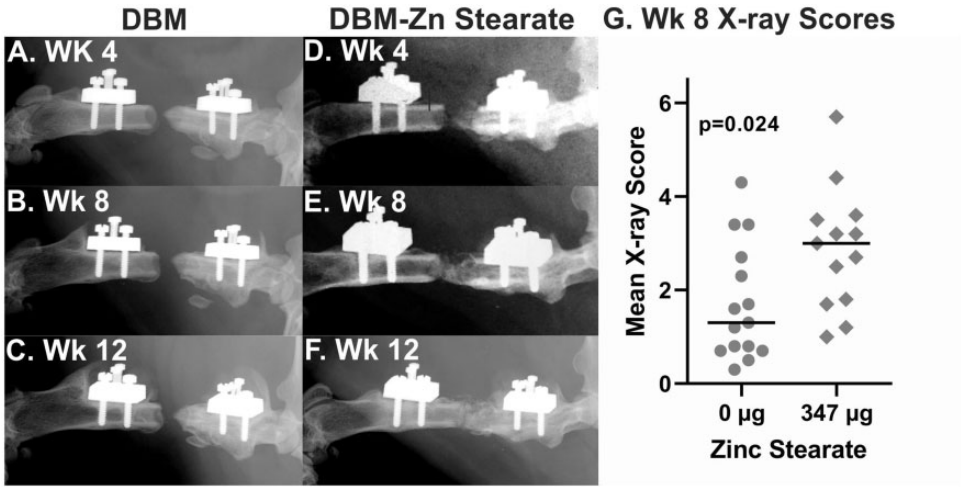

Figure 3. Improved femur defect osteogenesis in rats treated with DBM and zinc stearate. Serial radiographs at 4, 8, and 12 weeks show little calcified tissue in a defect site treated with DBM only (a to c) but abundant calcified tissue in a defect treated with DBM-Zn stearate (347 µg) (d to f). (g) Defect sites of rats treated with DBM-Zn stearate (347 µg) ($n = 13$) had significantly better radiograph scores at eight weeks than defect sites treated with DBM only ($n = 15$) ($P = 0.024$, nested t-test). DBM: demineralized bone matrix.

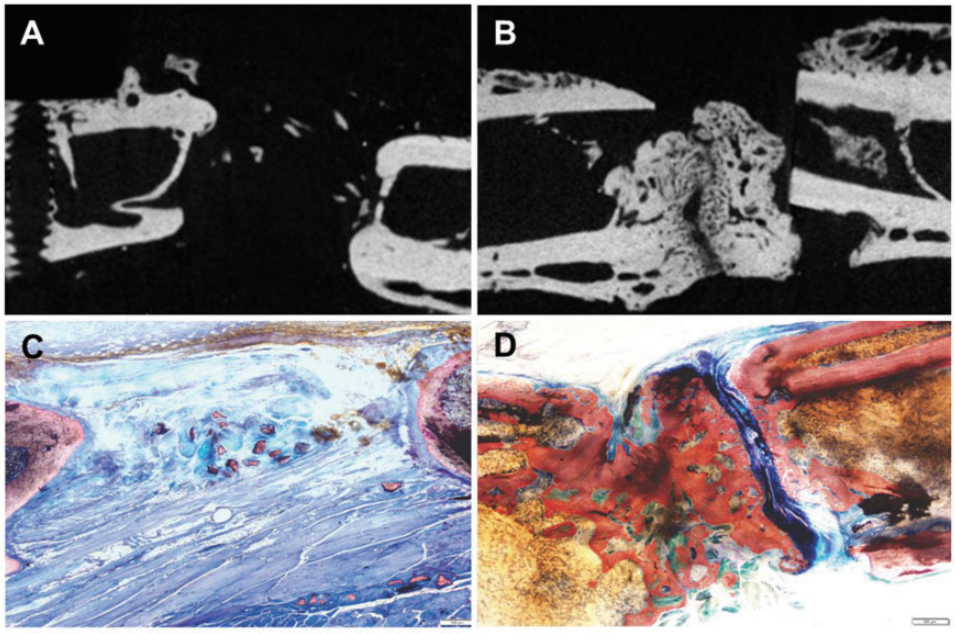

Figure 4. µCT and histology images of femur defects treated with DBM-Zn stearate (347 µg). µCT images of defect sites treated with DBM only (a) and DBM-Zn stearate (347 µg) (b). Defects treated with DBM only showed sparse new bone formation while abundant bone was evident in the defects of the DBM-Zn stearate (347 µg) treated defects. Corresponding histological sections of the DBM only (c) and DBM-Zn stearate (347 µg) treated defects (d) confirm bone formation within the DBM-Zn stearate (347 µg) treated defect. Scale bars are 500 µm. (A color version of this figure is available in the online journal.)

treated with DBM only showed only small islands of calcified tissue within the defect (Figure 4(a)). In contrast, a µCT image of a defect treated with DBM-Zn stearate (347 µg) showed abundant new bone present within the defect. In rats treated with DBM-Zn stearate (347 µg) ($n = 8$), mid-diaphyseal bone volume was greater than the mid-diaphyseal bone volume in rats treated with DBM only ($n = 6$; 112.2 vs. 83.6 mm^3; t-test, $P = 0.04$). Similarly, histological examination of specimens collected 12 weeks after surgery showed a robust bone formation response in defects treated with DBM-Zn stearate (347 µg) (Figure 4(c) and (d)).

Zinc binding and retention on morselized bone allograft

Binding of zinc to morselized bone allograft (bone chips) was concentration and time dependent. When bone chips were incubated in 0.01%, 0.1%, and 1% $ZnCl_2$ for 24 h, the amount of zinc bound to the bone chips increased significantly as the concentration of zinc in the solution increased (one-way ANOVA, $P < 0.001$, Figure 5(a)). When bone chips were soaked in 1% $ZnCl_2$, the amount of zinc bound significantly increased over time (ANOVA, $P < 0.001$, Figure 5(b)). Significant increases in the amount of zinc bound changed between 0 and 0.5 h, between 3 and 24 h, and between 24 and 96 h (Holm–Sidak, $P < 0.05$).

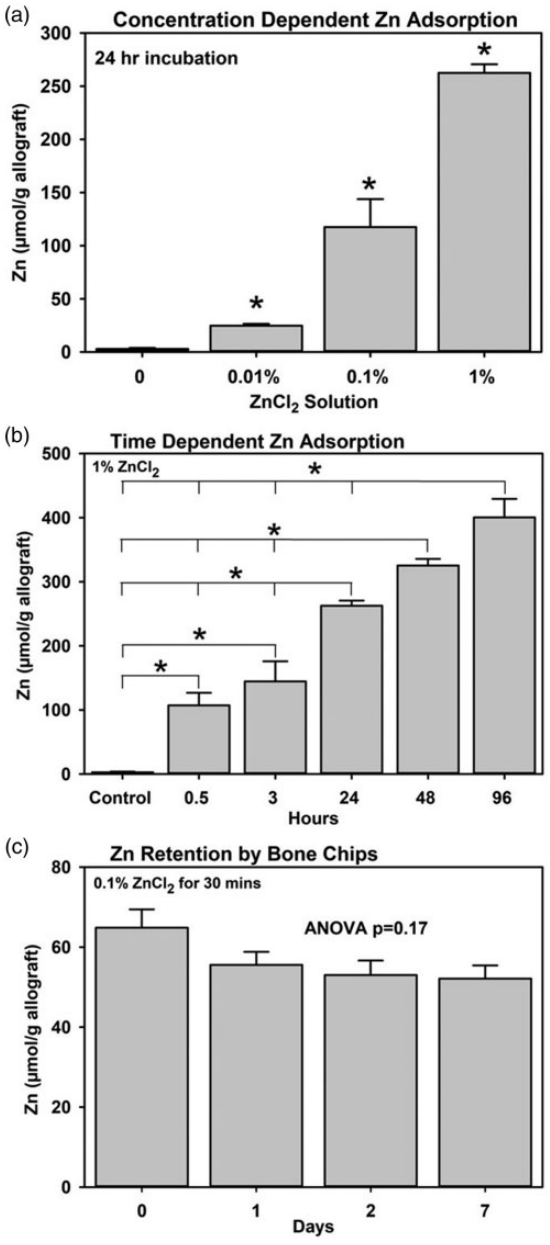

Figure 5. Zinc binding to morselized human bone allograft is concentration and time dependent. (a) Aliquots of morselized human bone allograft (bone chips) were incubated for 24 h in 0, 0.01, 0.1, and 1% $ZnCl_2$ for 24 h and then bound Zn was measured. The amount of Zn bound to the bone chips increased as the concentration of $ZnCl_2$ increased (*, Holm–Sidak, $P < 0.001$). (b) Bone chips were soaked in 1% $ZnCl_2$ for increasing times before the amount of bound Zn was measured. The amount of Zn bound increased continuously over the course of the experiment (*, Holm–Sidak, $P < 0.001$). (c) Zn bound to bone chips after 30 min incubation in 0.1% $ZnCl_2$ was retained with the bone chips for at least a week *in vitro* (one-way ANOVA, $P = 0.17$). ANOVA: analysis of variance.

Retention of zinc on bone chips was also measured. After incubating in 0.1% $ZnCl_2$ for 30 min, the bone chips were washed with TBS (0 time) before incubating in TBS for additional one, two, or seven days. Aliquots of bone chips collected at each time point were dissolved in nitric acid and the amount of Zn in the acid extract determined using ICP-MS. The initial amount of zinc bound to the bone chips was 64.8 ± 7.9 µmol/g of allograft. There was a 15% decrease in the mean amount of Zn bound after 24 h in TBS, and a further 5% decrease over the next six days was measured, but the differences were not significant (ANOVA, $P = 0.17$, Figure 5(c)).

Improved osteogenesis using zinc-treated morselized bone allograft

Zn-bound and untreated bone chips were tested in the rat femur defect model to determine whether Zn-bound bone chips would promote osteogenesis. Serial radiographs of rat defects filled with untreated and Zn-bound bone chips at 2, 8, and 12 weeks after surgery are shown in Figure 6. Unlike DBM, bone chips are calcified tissue and thus appear in the radiographs of the defect. The untreated bone chips appear to become more radiolucent over time as compared to the Zn-bound bone chips. There also appears to be more new bone formed in the defect of the rat treated with the Zn-bound bone chips.

Histological sections and µCT images of defects treated with Zn-bound bone chips confirmed the presence of new bone formation in the defect (Figure 7(a) to (d)). Isolated and irregularly shaped areas of calcified tissue were present in the defect filled with untreated bone chips after 12 weeks of healing and may represent remnants of the implanted allograft (Figure 7(a) and (b)). Conversely, the calcified tissue present within the defect filled with Zn-bound bone chips showed areas of new bone formation and an organized structure spanning the defect after 12 weeks of healing (Figure 7(c) and (d)).

Histomorphometric and µCT analyses found significantly more calcified tissue in the defect of the rats filled with the Zn-bound bone chips. Histomorphometry measured over 2.5 times more calcified tissue in the defects filled with Zn-bound bone chips as compared to the defects filled with untreated bone chips (14.5 vs. 5.3 mm^2, Mann–Whitney, $P = 0.029$, Figure 7(e)). Similarly, defects filled with Zn-bound bone chips had significantly greater volume of calcified tissue in the defect than the defects filled with untreated bone chips (125.8 vs. 82.4 mm^3, *t*-test, $P = 0.03$, Figure 7(f)).

Effect of Zn on skeletal cell proliferation and viability

Unlike DBM-$ZnCl_2$ (75 µg), we observed no positive effect on osteogenesis when *Rag2* null rat femur defects were treated with DBM-$ZnCl_2$ (150 µg) or DBM-$ZnCl_2$ (300 µg) in preliminary experiments (data not shown). These preliminary observations suggest that $ZnCl_2$ may have dose-limiting effects on bone formation and that Zn may be cytotoxic at high concentrations. To assess the potential cytotoxicity, the effects of different Zn concentrations and salts on skeletal cell proliferation and viability were measured. Murine RAW264.7, MC3T3-E1, and ATDC5 cell lines were used as models for preosteoclasts, osteoblasts, and chondrocytes, respectively.[26–28] The cells were cultured in media supplemented with increasing amounts of $ZnCl_2$ or with different soluble salts of zinc. For all cell lines and for all zinc salts tested, no viable cells were detected after two, four, or seven days in culture when Zn salts were added to 300 µM (data not

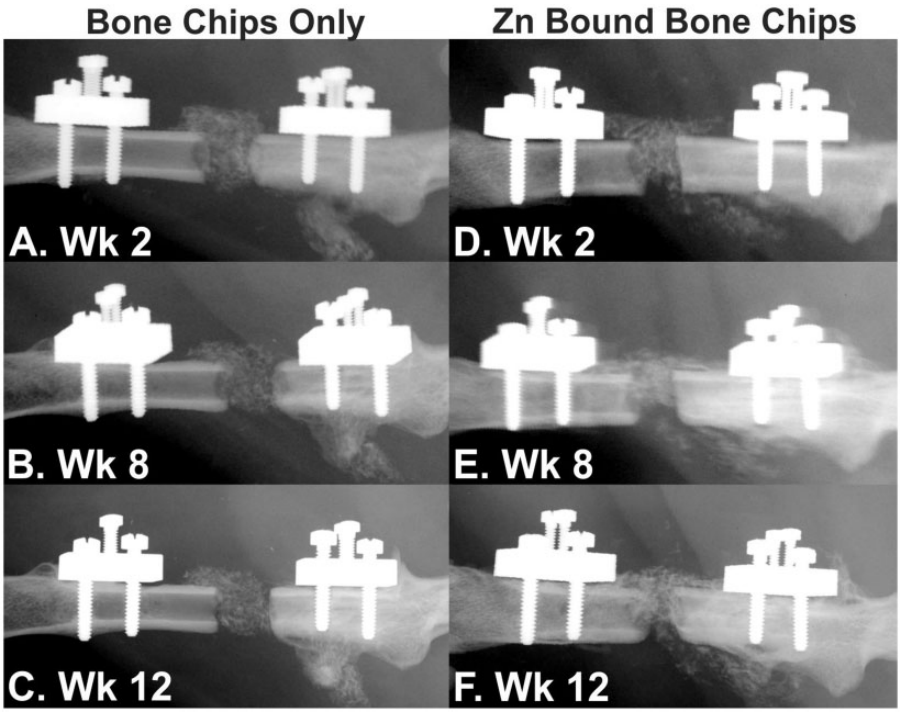

Figure 6. Serial radiographs of rat femur defects treated with morselized human bone allograft. Serial radiographs taken at 2 (a and d), 8 (b and e), and 12 weeks (c and f) after surgery are shown. Little or no new bone formation was observed in the defect filled with bone chips only (a to c). The bone chips also appeared to decrease in radio-opacity over time. In contrast, new bone formation was evident in the defect filled with Zn-bound bone chips (d to f). Furthermore, the Zn-bound bone chips appeared to remain radio-opaque over the course of the experiment.

shown). At 100 μM or less, $ZnCl_2$ had no effect on RAW264.7 cell proliferation or viability (Figure 8(a) and (d)). For MC3T3-E1 cells, 100 μM $ZnCl_2$ decreased viability to 92.4% after two days as compared to 98.2% in control cultures (Holm–Sidak, $P = 0.008$). However, 100 μM $ZnCl_2$ had no significant effect on proliferation or viability on MC3T3-E1 cells after seven days in culture despite the apparent reduction in number of viable cells at day 7 (Figure 8(b) and (e)). For ATDC5 cells, 30 and 100 μM $ZnCl_2$ significantly lowered the increase in viable cells at day 7 compared to control (Holm–Sidak, $P \leq 0.02$, Figure 8(c)) and 100 μM $ZnCl_2$ decreased cell viability by day 7 (Holm–Sidak, $P = 0.013$, Figure 8(f)).

The effect of other soluble zinc salts on skeletal cell viability was also tested. Each salt was tested at 100 μM and the percentage of viable RAW264.7, MC3T3-E1, and ATDC5 cells was measured after two and seven days in culture (Figure 8(d) to (f)). Zinc citrate was toxic to all cell types with no viable cells detected after two or seven days in culture. Zinc acetate dramatically reduced ATDC5 cell viability to 23.5% after just two days in culture (Holm–Sidak, $P \leq 0.001$) and RAW264.7 cell viability to 12.4% after seven-days in culture (Holm–Sidak, $P \leq 0.001$). Zinc acetate reduced the viability of MC3T3-E1 cells to 94.0% after two-days in culture (Holm–Sidak, $P = 0.039$) and to 75.2% after seven days in culture (Holm–Sidak, $P = 0.039$). Zinc sulfate had no significant effect on the viability of RAW264.7 or MC3T3-E1 cells but dramatically reduced the percentage of viable ATDC5 cells to 24.2% after seven days in culture (Holm–Sidak, $P \leq 0.001$).

Discussion

The study found that allograft supplemented with Zn could produce a better bone formation response than allograft alone. Using the rat femoral segmental defect model, defects treated with 60 mgs of DBM supplemented with 0.55 μmol of Zn as either $ZnCl_2$ (75 μg) or Zn stearate (347 μg) showed enhanced bone formation as early as six weeks postsurgery. Histomorphometric and μCT assessments also showed quantitative enhancements in bone formation after 12 weeks in defects treated with DBM and a Zn adjuvant. The dose of Zn used equates to 9.2 μmol Zn/g DBM or 0.06% w/w of Zn to DBM. Use of Zn-bound morselized bone allograft (bone chips) to treat the rat femur defects also showed enhanced bone formation via μCT and histomorphometric analyses. However, the Zn-bound bone chips used to treat the rat femur defects were calculated to contain 35 μmol of Zn/g bone chips or 0.23% w/w of Zn to allograft or four times the amount Zn used with the DBM.

Osteogenic effects of zinc in bone regeneration appeared to occur within a narrow dose range when used as an adjuvant with DBM. While DBM-$ZnCl_2$ (75 μg) enhanced bone regeneration, larger doses of $ZnCl_2$ appeared to have no beneficial effect (not shown). Prior studies tested the *in vivo* osteogenic effects of incorporating Zn into various synthetic graft materials, such as tricalcium phosphate and hydroxyapatite, or use of Zn containing metal alloys.[17] The results of the prior studies are difficult to compare since synthetic graft materials, graft preparation, Zn dose,

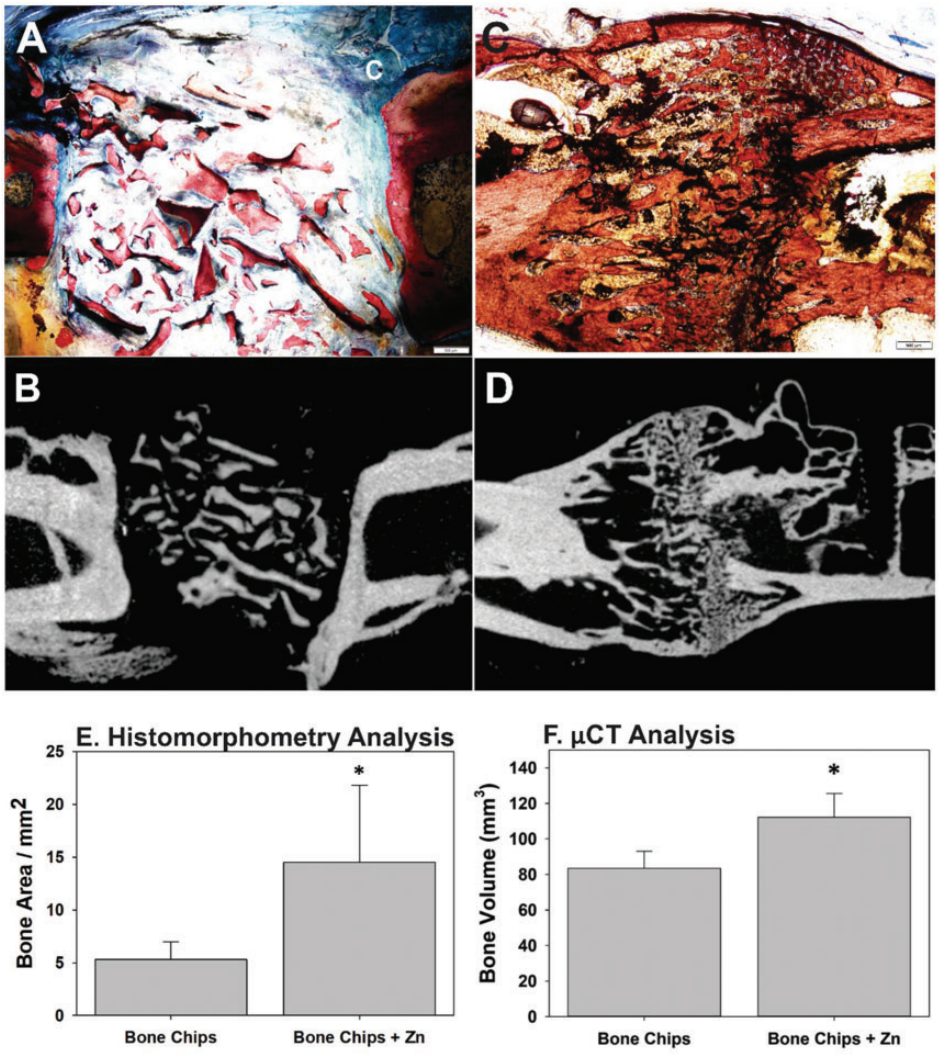

Figure 7. Histological and μCT analysis of rat femur defects treated with bone allograft. Histology (a) and μCT (b) images for a defect treated with bone chips only showed minimal new bone formation. Histology (c) and μCT (d) images of a defect treated with zinc-bound bone chips showed plentiful new bone formation in and around the defect site. Scale bar is 500 μm. (e) Histomorphometry showed a significant increase in defect site bone area for those defects treated with Zn-bound bone chips ($n = 7$) as compared to defects treated with bone chips only ($n = 6$; *Mann–Whitney, $P = 0.029$) after 12 weeks of healing. (f) μCT analysis found significantly more bone in defects treated with Zn-bound bone chips ($n = 11$) than those treated with bone chips only ($n = 11$, *t-test, $P = 0.04$) after 12 weeks of healing. μCt: micro-computed tomography. (A color version of this figure is available in the online journal.)

and animal models varied between studies. However, Kawamura *et al*., using tricalcium phosphate and hydroxyapatite composites (TCP/HA) sintered with Zn, found that the TCP/HA implants containing 0.3% by weight Zn produced a significant increase in osteoconductive bone formation in a rabbit femur diaphyseal, bi-cortical, drill-hole defect than TCP/HA implants with 0, 0.06, or 0.6% by weight Zn.[29] Krell *et al*., using a calcium sulfate paste as a carrier, found that an intramedullary dose of 1 mg/kg $ZnCl_2$ ($ZnCl_2$ to body weight) significantly improved rat femur fracture healing as compared to a 3 mg/kg dose of $ZnCl_2$.[15]

Results from the *in vitro* proliferation and cytotoxicity assays also support the conclusion that Zn has dose-limiting effects on promoting osteogenesis. Zn has anti-bacterial, anti-inflammatory, anti-oxidant, and pro-osteogenic effects as described in prior studies.[30–32] However, high levels of Zn can also be cytotoxic. Using well-characterized mouse cell lines, we found that the cytotoxic effects of Zn were concentration, salt, and cell dependent. For instance, ATDC5 cell proliferation was inhibited at 30 and 100 μM $ZnCl_2$, while 300 μM $ZnCl_2$ was cytotoxic. Furthermore, 100 μM Zn acetate significantly reduced ATDC5 cell viability, indicating a significant counter-ion effect. The effects of $ZnCl_2$, Zn acetate, and Zn sulfate on RAW264.7 and MC3T3-E1 cells were generally not as pronounced as the effects observed with ATDC5 cells, but 300 μM $ZnCl_2$ and 100 μM Zn citrate were cytotoxic for all cell lines. Other studies also found that Zn can cause cytotoxicity. For instance, Srivastava *et al*. found that 600 μM or 900 μM of Zn nitrate was cytotoxic to C3H10T$_{1/2}$ cells while concentrations $\leq$300 μM had no effect on cell viability.[33] The present study did not address Zn effects on osteoblast activity, chondrogenesis, or osteoclastogenesis. However, Cho and Kwun found that 15 μM but not 1 μM could promote osteogenic gene expression in

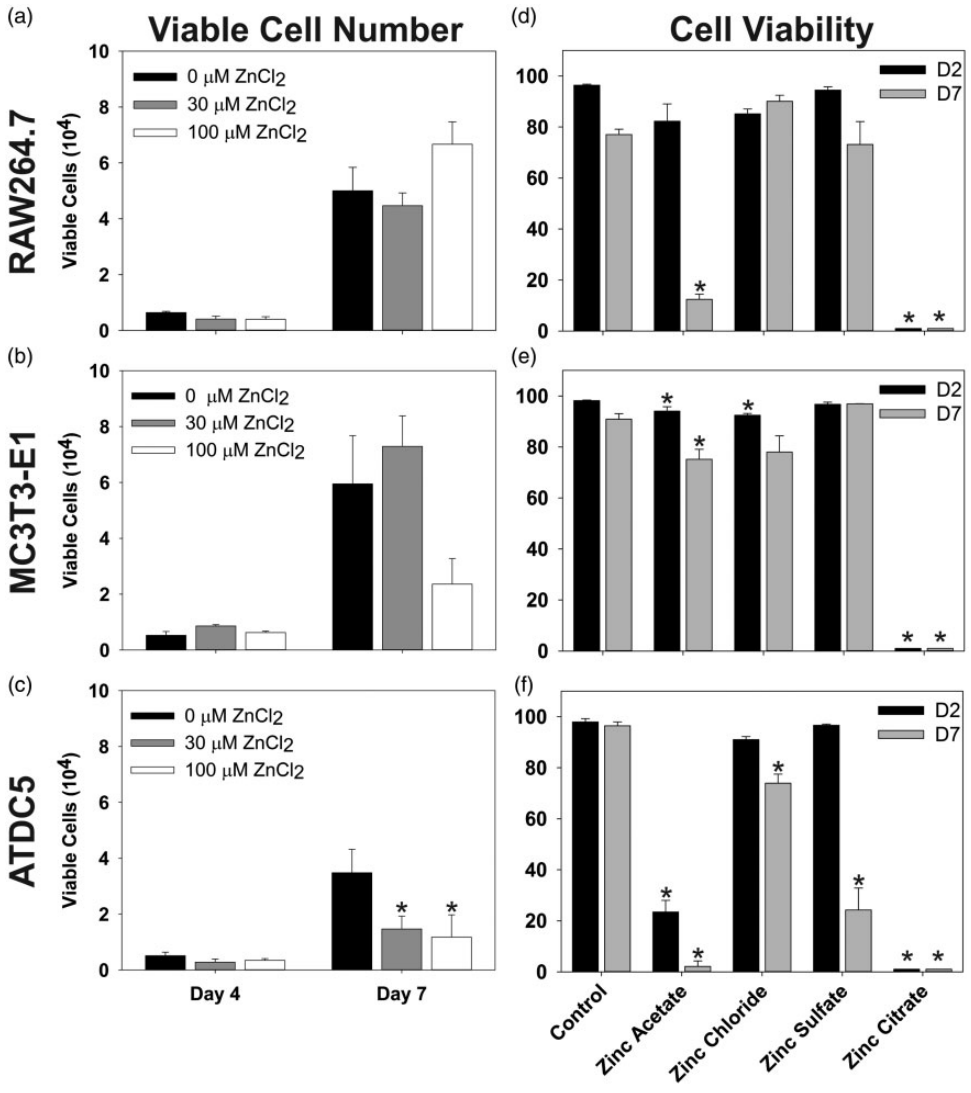

Figure 8. Effect of Zn on cell proliferation and viability. (a to c) RAW264.7, MC3T3-E1, and ATDC5 cells were cultured in media containing increasing concentrations of $ZnCl_2$ (0, 30, and 100 μM: black, gray, and white, respectively). Viable cells were counted after four and seven days in culture. Bars represent mean values (+SE) from three cell cultures measured for each treatment. Moreover, 300 μM of $ZnCl_2$ was toxic to all cell types at four and seven days (not shown). RAW264.7 cells were not affected (a). The mean number of MC3T3-E1 cells after seven days in culture was not significantly different from the control value (b). 30 and 100 μM $ZnCl_2$ reduced the increase in the number of viable ATDC5 cells as compared to the control ATDC5 cultures after seven days in culture ($P < 0.02$, c). The effects of different zinc salts at 100 μM on the viability of RAW264.7 (d), MC3T3-E1 (e), and ATDC5 (f) cells was measured after two (black bars) and seven days (gray bars) in culture. Bars represent mean values (+SE) from three cultures measured for each cell line, time point, and salt. In cultures containing zinc citrate, no viable cells were detected. Zinc acetate reduced RAW264.7 cell viability after 7 days in culture (d, $P \leq 0.001$) and ATDC5 cell viability after two and seven days in culture (f, $P \leq 0.001$). Zinc acetate after two and seven days and zinc chloride after two days in culture had modest effects on MC3T3-E1 cell viability (e, $P = 0.039$, 0.039, and 0.008, respectively). Zinc sulfate and to a lesser extent, zinc chloride, also reduced ATDC5 cell viability after seven days in culture (f, $P \leq 0.001$ and 0.013, respectively).

MC3T3-E1 cells.[34] Thus, *in vitro* and *in vivo* studies indicate that the beneficial effects of Zn on osteogenesis are dose-limiting.

Soluble Zn levels at the site of bone formation also appear to be an important factor for determining Zn dose. DBM supplemented with Zn stearate (DBM-Zn stearate [347 μg]) appeared to produce a more consistent osteogenic response than DBM-$ZnCl_2$ (75 μg) in the rat femur defect model based on radiographic scoring. As Zn stearate is not water soluble, Zn release from Zn stearate into the defect site may have been slowed by the stearate counter ion, which could potentially account for the apparent better osteogenic response. The Zn-bound bone chips used in the study delivered four times more Zn to the femur defect site than DBM-$ZnCl_2$ (75 μg), yet the Zn-bound chips were still effective at promoting bone formation, whereas DBM supplemented with two (150 μg) or four times (300 μg) more $ZnCl_2$ did not appear to be effective in preliminary experiments. *In vitro*, Zn was retained on the bone chips for at least seven days. Together, these observations indicate that Zn release kinetics from the implanted allograft material, or likely any carrier, can significantly impact the ability of Zn to promote osteogenesis.

Based on the apparent dose-limiting effects of Zn on bone formation, use of Zn as an adjuvant to enhance or promote bone regeneration will require a better understanding of how Zn dose and delivery can optimize osteogenesis. Optimization will require use of standardized

animal models to control for host variables since the optimal Zn dose may relate to animal body size, skeletal site, target bone defect volume, and perhaps target defect bone area. Since Zn preferentially localizes to bone,[35] the optimal Zn dose may relate to available bone surface area to which the Zn may localize at the site of bone regeneration. Further optimization could involve choice of Zn salt used and choice of carriers to deliver Zn as a bolus dose or over an extended time depending on the target environment, such as treating a segmental defect versus promoting posterolateral spinal fusion.

The mechanisms by which zinc enhances bone regeneration remain unclear. Zn is a trace metal normally present in bone and allograft processing can reduce the amount of Zn maintained in the bone matrix. Thus, use of Zn as an allograft adjuvant may improve allograft osteogenic capacity by restoring the allograft to a more physiological state. Zn is also a co-factor for many structural and catalytic proteins including carbonic anhydrase, alkaline phosphatase, matrix metalloproteases, histone deacetylases, and zinc-finger transcription factors.[36,37] As such, dietary or genetic Zn insufficiency can affect many signaling, metabolic, and physiological pathways including skeletal homeostasis.[38–41] Perhaps because Zn affects so many proteins, signaling pathways, and physiological responses, how excess Zn can promote osteogenesis is unclear. Prior *in vitro* studies have shown that Zn can promote mesenchymal stem cell differentiation to osteoblasts[42,43] and enhance osteoblast activity by increasing BMP-2 expression, SMAD-1 activation, and *Runx2* expression.[34] Kirkpatrick *et al*. found that chondrocyte proliferation, through AKT activation, was enhanced by 50 μM Zn.[44] Zn can also inhibit osteoclastogenesis and promote osteoclast apoptosis.[45,46] *In vivo*, a prior rat femur fracture healing study found that Zn applied at the fracture site increased callus cartilage and promoted fracture healing.[15] Thus, the available evidence indicates that Zn promotes bone regeneration by promoting anabolic while inhibiting catabolic processes during osteogenesis.

To our knowledge, this was the first time a critical-sized femoral defect model was used in *Rag2* null rats.[47] A significant loss of experimental animals occurred during the study. The primary cause of lost animals was from fixation failure associated with screw pull-outs or cortical bone cracking with 22% of all study animals being lost from fixation failure by four weeks after surgery. A preliminary assessment of the male *Rag2* null rat bone quality found that the intrinsic material properties of the femurs (maximum shear stress and shear modulus) were similar to that of femurs from female Sprague-Dawley rats, suggesting that initial bone quality may not have been the cause of the high fixation failure rate. *Rag2* null rats lack B and T cells and prior studies have shown the importance of B and T cells in bone metabolism.[48–50] The lack of an intact immune system permitted testing of human bone allograft with Zn adjuvants in the *Rag2* null rat model, but whether the lack of an intact immune response affected the osteogenic activity of Zn or affected fixation failure rates will require further investigation.

Conclusions

The study results support the use of Zn as an osteogenic adjuvant for allograft. Increasing the osteogenic capacity of allograft with Zn should improve clinical outcomes and reduce healing complications associated with vulnerable patient populations. Continued development of Zn as a therapeutic adjuvant will require a better understanding of dose–response relationships and the osteogenic mechanism of action.

AUTHORS' CONTRIBUTIONS

DK performed *in vivo* experiments, data analysis, and prepared the manuscript. CG performed *in vitro* experiments and data analysis. MDC assisted with animal surgeries and histology. SSL, MV, and JB assisted in method development and data interpretation. JPOC designed the study, performed data analysis and interpretation, prepared the manuscript, and supervised the project. All authors participated in the review and editing of the manuscript.

ACKNOWLEDGEMENTS

The investigators thank the Miami Tissue Bank for donating the morselized bone allograft and Dr. Jeffrey Cartmell and the Musculoskeletal Transplant Foundation for donating the demineralized bone matrix. The authors thank Yazan Kadkoy and Alison Caceres for their contributions in the animal surgeries and histological processing.

DECLARATION OF CONFLICTING INTERESTS

DK, CG, and MDC have no conflicts of interest. SSL, MV, JB, and JPOC are inventors on patents related to this technology. SSL, MV, and JB are partial owners of CreOsso LLC which has licensed technology from Rutgers University to develop osteogenic therapies related to the technology described in this manuscript.

FUNDING

The author(s) disclosed receipt of the following financial support for the research, authorship, and/or publication of this article: This work was supported by the Musculoskeletal Transplant Foundation and the National Institute of Arthritis and Musculoskeletal and Skin Diseases of the National Institutes of Health (R01AR069044).

ORCID iD

J Patrick O'Connor https://orcid.org/0000-0003-0282-1104

SUPPLEMENTAL MATERIAL

Supplemental material for this article is available online.

REFERENCES

1. Muscolo DL, Ayerza MA, Aponte-Tinao L, Ranalletta M, Abalo E. Intercalary femur and tibia segmental allografts provide an acceptable alternative in reconstructing tumor resections. *Clin Orthop Relat Res* 2004;**426**:97–102

2. Muscolo DL, Ayerza MA, Aponte-Tinao LA, Ranalletta M. Partial epiphyseal preservation and intercalary allograft reconstruction in high-grade metaphyseal osteosarcoma of the knee. *J Bone Joint Surg* 2005;**87**:226–36
3. Ekegren CL, Edwards ER, de Steiger R, Gabbe BJ. Incidence, costs and predictors of non-union, delayed union and mal-union following long bone fracture. *Int J Environ Res Public Health* 2018;**15**:2845
4. Kan SL, Yuan ZF, Ning GZ, Yang B, Li HL, Sun JC, Feng SQ. Autograft versus allograft in anterior cruciate ligament reconstruction: a meta-analysis with trial sequential analysis. *Medicine* 2016;**95**:e4936
5. Sohn HS, Oh JK. Review of bone graft and bone substitutes with an emphasis on fracture surgeries. *Biomater Res* 2019;**23**:9
6. Katz JM, Nataraj C, Jaw R, Deigl E, Bursac P. Demineralized bone matrix as an osteoinductive biomaterial and in vitro predictors of its biological potential. *J Biomed Mater Res B Res* 2009;**89**:127–34
7. Galindo-Moreno P, de Buitrago JG, Padial-Molina M, Fernandez-Barbero JE, Ata-Ali J, O' Valle F. Histopathological comparison of healing after maxillary sinus augmentation using xenograft mixed with autogenous bone versus allograft mixed with autogenous bone. *Clin Oral Impl Res* 2018;**29**:192–201
8. Mankin HJ, Gebhardt MC, Jennings LC, Springfield DS, Tomford WW. Long-term results of allograft replacement in the management of bone tumors. *Clin Orthop Relat Res* 1996;**324**:86–97
9. Donati D, Di Liddo M, Zavatta M, Manfrini M, Bacci G, Picci P, Capanna R, Mercuri M. Massive bone allograft reconstruction in high-grade osteosarcoma. *Clin Orthop Relat Res* 2000;**377**:186–94
10. Deijkers RL, Bloem RM, Kroon HM, Van Lent JB, Brand R, Taminiau AH. Epidiaphyseal versus other intercalary allografts for tumors of the lower limb. *Clin Orthop Relat Res* 2005;**439**:151–60
11. Farid Y, Lin PP, Lewis VO, Yasko AW. Endoprosthetic and allograft-prosthetic composite reconstruction of the proximal femur for bone neoplasms. *Clin Orthop Relat Res* 2006;**442**:223–9
12. Fox EJ, Hau MA, Gebhardt MC, Hornicek FJ, Tomford WW, Mankin HJ. Long-term followup of proximal femoral allografts. *Clin Orthop Relat Res* 2002;**397**:106–13
13. Hornicek FJ, Gebhardt MC, Tomford WW, Sorger JI, Zavatta M, Menzner JP, Mankin HJ. Factors affecting nonunion of the allograft-host junction. *Clin Orthop Relat Res* 2001;**382**:87–98
14. Ortiz-Cruz E, Gebhardt MC, Jennings LC, Springfield DS, Mankin HJ. The results of transplantation of intercalary allografts after resection of tumors. A long-term follow-up study. *J Bone and Joint Surg* 1997;**79**:97–106
15. Krell ES, Ippolito JA, Montemurro NJ, Lim PH, Vincent RA, Hreha J, Cottrell J, Sudah SY, Munoz MF, Pacific KP, Benevenia J, O'Connor JP, Lin SS. Local zinc chloride release from a calcium sulfate carrier enhances fracture healing. *J Orthop Trauma* 2017;**31**:168–74
16. Wey A, Cunningham C, Hreha J, Breitbart E, Cottrell J, Ippolito J, Clark D, Lin HN, Benevenia J, O'Connor JP, Lin SS, Paglia DN. Local $ZnCl_2$ accelerates fracture healing. *J Orthop Res* 2014;**32**:834–41
17. O'Connor JP, Kanjilal D, Teitelbaum M, Lin SS, Cottrell JA. Zinc as a therapeutic agent in bone regeneration. *Materials (Basel, Switzerland)* 2020;**13**:2211
18. Oest ME, Dupont KM, Kong HJ, Mooney DJ, Guldberg RE. Quantitative assessment of scaffold and growth factor-mediated repair of critically sized bone defects. *J Orthop Res* 2007;**25**:941–50
19. Boerckel JD, Dupont KM, Kolambkar YM, Lin AS, Guldberg RE. In vivo model for evaluating the effects of mechanical stimulation on tissue-engineered bone repair. *Journal of Biomechanical Engineering* 2009;**131**:084502
20. Subramanian S, Mitchell A, Yu W, Snyder S, Uhrich K, O'Connor JP. Salicylic acid-based polymers for guided bone regeneration using bone morphogenetic protein-2. *Tissue Eng Part A* 2015;**21**:2013–24
21. Yassine KA, Mokhtar B, Houari H, Karim A, Mohamed M. Repair of segmental radial defect with autologous bone marrow aspirate and hydroxyapatite in rabbit radius: a clinical and radiographic evaluation. *Vet World* 2017;**10**:752–7
22. Bodde EW, Kowalski RS, Spauwen PH, Jansen JA. No increased bone formation around alendronate or omeprazole loaded bioactive bone cements in a femoral defect. *Tissue Eng Part A* 2008;**14**:29–39
23. Maniatopoulos C, Rodriguez A, Deporter DA, Melcher AH. An improved method for preparing histological sections of metallic implants. *Int J Oral Maxillofac Implants* 1986;**1**:31–7
24. Baron R, Vigney A, Neff L, Silvergate A, Santa MA. Processing of undecalcified bone specimens for bone histomorphometry. In: RR Recker (ed.) *Bone histomorphometry: techniques and interpretation*. Boca Raton: CRC Press, Inc., 1983, pp. 13–35
25. Harten RD, Svach DJ, Schmeltzer R, Uhrich KE. Salicylic acid-derived poly(anhydride-esters) inhibit bone resorption and formation in vivo. *J Biomed Mater Res A* 2005;**72**:354–62
26. Hsu H, Lacey DL, Dunstan CR, Solovyev I, Colombero A, Timms E, Tan HL, Elliott G, Kelley MJ, Sarosi I, Wang L, Xia XZ, Elliott R, Chiu L, Black T, Scully S, Capparelli C, Morony S, Shimamoto G, Bass MB, Boyle WJ. Tumor necrosis factor receptor family member RANK mediates osteoclast differentiation and activation induced by osteoprotegerin ligand. *Proc Natl Acad Sci U S A* 1999;**96**:3540–5
27. Sudo H, Kodama HA, Amagai Y, Yamamoto S, Kasai S. In vitro differentiation and calcification in a new clonal osteogenic cell line derived from newborn mouse calvaria. *J Cell Biol* 1983;**96**:191–8
28. Atsumi T, Miwa Y, Kimata K, Ikawa Y. A chondrogenic cell line derived from a differentiating culture of AT805 teratocarcinoma cells. *Cell Differ Dev* 1990;**30**:109–16
29. Kawamura H, Ito A, Miyakawa S, Layrolle P, Ojima K, Ichinose N, Tateishi T. Stimulatory effect of zinc-releasing calcium phosphate implant on bone formation in rabbit femora. *J Biomed Mater Res* 2000;**50**:184–90
30. Horky P, Skalickova S, Urbankova L, Baholet D, Kociova S, Bytesnikova Z, Kabourkova E, Lackova Z, Cernei N, Gagic M, Milosavljevic V, Smolikova V, Vaclavkova E, Nevrkla P, Knot P, Krystofova O, Hynek D, Kopel P, Skladanka J, Adam V, Smerkova K. Zinc phosphate-based nanoparticles as a novel antibacterial agent: in vivo study on rats after dietary exposure. *J Anim Sci Biotechnol* 2019;**10**:17
31. Jarosz M, Olbert M, Wyszogrodzka G, Myniec K, Librowski T. Antioxidant and anti-inflammatory effects of zinc. Zinc-dependent NF-κB signaling. *Inflammopharmacol* 2017;**25**:11–24
32. Yu J, Xu L, Li K, Xie N, Xi Y, Wang Y, Zheng X, Chen X, Wang M, Ye X. Zinc-modified calcium silicate coatings promote osteogenic differentiation through TGF-beta/smad pathway and osseointegration in osteopenic rabbits. *Sci Rep* 2017;**7**:3440
33. Srivastava S, Kumar N, Thakur RS, Roy P. Role of vanadium (V) in the differentiation of C3H10t1/2 cells towards osteoblast lineage: a comparative analysis with other trace elements. *Biol Trace Elem Res* 2013;**152**:135–42
34. Cho Y-E, Kwun I-S. Zinc upregulates bone-specific transcription factor Runx2 expression via BMP-2 signaling and smad-1 phosphorylation in osteoblasts. *J Nutr Health* 2018;**51**:23–30
35. Zhang SQ, Yu XF, Zhang HB, Peng N, Chen ZX, Cheng Q, Zhang XL, Cheng SH, Zhang Y. Comparison of the oral absorption, distribution, excretion, and bioavailability of zinc sulfate, zinc gluconate, and zinc-enriched yeast in rats. *Mol Nutr Food Res* 2018;**62**:e1700981
36. Vallee BL, Auld DS. Zinc coordination, function, and structure of zinc enzymes and other proteins. *Biochemistry* 1990;**29**:5647–59
37. Andreini C, Bertini I. A bioinformatics view of zinc enzymes. *J Inorg Biochem* 2012;**111**:150–6
38. Jovanovic M, Schmidt FN, Guterman-Ram G, Khayyeri H, Hiram-Bab S, Orenbuch A, Katchkovsky S, Aflalo A, Isaksson H, Busse B, Jahn K, Levaot N. Perturbed bone composition and integrity with disorganized osteoblast function in zinc receptor/Gpr39-deficient mice. *Faseb J* 2018;**32**:2507–18
39. Kambe T, Tsuji T, Hashimoto A, Itsumura N. The physiological, biochemical, and molecular roles of zinc transporters in zinc homeostasis and metabolism. *Physiol Rev* 2015;**95**:749–84
40. Fukada T, Hojyo S, Furuichi T. Zinc signal: a new player in osteobiology. *J Bone Miner Metab* 2013;**31**:129–35
41. Inoue K, Matsuda K, Itoh M, Kawaguchi H, Tomoike H, Aoyagi T, Nagai R, Hori M, Nakamura Y, Tanaka T. Osteopenia and male-specific sudden cardiac death in mice lacking a zinc transporter gene, Znt5. *Hum Mol Genet* 2002;**11**:1775–84

42. Shen X, Hu Y, Xu G, Chen W, Xu K, Ran Q, Ma P, Zhang Y, Li J, Cai K. Regulation of the biological functions of osteoblasts and bone formation by Zn-incorporated coating on microrough titanium. *ACS Appl Mater Interfaces* 2014;**6**:16426–40
43. Hu T, Xu H, Wang C, Qin H, An Z. Magnesium enhances the chondrogenic differentiation of mesenchymal stem cells by inhibiting activated macrophage-induced inflammation. *Sci Rep* 2018;**8**:3406
44. Kirkpatrick CJ, Mohr W, Haferkamp O. Influence of zinc and copper on lapine articular chondrocytes in monolayer culture: morphology, proliferation and proteoglycan synthesis. *Exp Cell Biol* 1982;**50**:108–14
45. Yamaguchi M, Weitzmann MN. Zinc stimulates osteoblastogenesis and suppresses osteoclastogenesis by antagonizing NF-kappaB activation. *Mol Cell Biochem* 2011;**355**:179–86
46. Yamada Y, Ito A, Kojima H, Sakane M, Miyakawa S, Uemura T, LeGeros RZ. Inhibitory effect of Zn2+ in zinc-containing beta-tricalcium phosphate on resorbing activity of mature osteoclasts. *J Biomed Mater Res A* 2008;**84**:344–52
47. Noto FK, Adjan-Steffey V, Tong M, Ravichandran K, Zhang W, Arey A, McClain CB, Ostertag E, Mazhar S, Sangodkar J, DiFeo A, Crawford J, Narla G, Jamling TY. Sprague dawley Rag2-Null rats created from engineered spermatogonial stem cells are immunodeficient and permissive to human xenografts. *Mol Cancer Ther* 2018;**17**:2481–9
48. Li Y, Toraldo G, Li A, Yang X, Zhang H, Qian WP, Weitzmann MN. B cells and T cells are critical for the preservation of bone homeostasis and attainment of peak bone mass in vivo. *Blood* 2007;**109**:3839–48
49. Mori G, D'Amelio P, Faccio R, Brunetti G. The interplay between the bone and the immune system. *Clin Dev Immunol* 2013;**2013**:720504
50. El Khassawna T, Serra A, Bucher CH, Petersen A, Schlundt C, Könnecke I, Malhan D, Wendler S, Schell H, Volk HD, Schmidt-Bleek K, Duda GN. T lymphocytes influence the mineralization process of bone. *Front Immunol* 2017;**8**:562

(Received January 8, 2021, Accepted May 3, 2021)